UC Berkeley

Title

Hybridization and Transgressive Evolution Generate Diversity in an Adaptive Radiation of Anolis Lizards.

Permalink

https://escholarship.org/uc/item/6zx5b9tw

Journal

Authors

Wogan, Guinevere
Yuan, Michael
Mahler, D
et al.

Publication Date

2023-08-07

DOI

Peer reviewed

Hybridization and Transgressive Evolution Generate Diversity in an Adaptive Radiation of *Anolis* Lizards

Guinevere O. U. Wogan[1,2,3], Michael L. Yuan[1,2], D. Luke Mahler[4], and Ian J. Wang[1,2,*],

[1]Department of Environmental Science, Policy, and Management, University of California, Berkeley, CA 94720, USA
[2]Museum of Vertebrate Zoology, University of California, Berkeley, CA 94720, USA
[3]Department of Integrative Biology, Oklahoma State University, Stillwater, OK 74078, USA and
[4]Department of Ecology and Evolutionary Biology, University of Toronto, Toronto, ON M5S 1A1, Canada
*Correspondence to be sent to: 54 Mulford Hall #3114, University of California, Berkeley, CA 94720-3114, USA; E-mail: ianwang@berkeley.edu.

Abstract.—Interspecific hybridization may act as a major force contributing to the evolution of biodiversity. Although generally thought to reduce or constrain divergence between 2 species, hybridization can, paradoxically, promote divergence by increasing genetic variation or providing novel combinations of alleles that selection can act upon to move lineages toward new adaptive peaks. Hybridization may, then, play a key role in adaptive radiation by allowing lineages to diversify into new ecological space. Here, we test for signatures of historical hybridization in the *Anolis* lizards of Puerto Rico and evaluate 2 hypotheses for the role of hybridization in facilitating adaptive radiation—the *hybrid swarm origins* hypothesis and the *syngameon* hypothesis. Using whole genome sequences from all 10 species of Puerto Rican anoles, we calculated D and *f*-statistics (from ABBA-BABA tests) to test for introgression across the radiation and employed multispecies network coalescent methods to reconstruct phylogenetic networks that allow for hybridization. We then analyzed morphological data for these species to test for patterns consistent with transgressive evolution, a phenomenon in which the trait of a hybrid lineage is found outside of the range of its 2 parents. Our analyses uncovered strong evidence for introgression at multiple stages of the radiation, including support for an ancient hybrid origin of a clade comprising half of the extant Puerto Rican anole species. Moreover, we detected significant signals of transgressive evolution for 2 ecologically important traits, head length and toepad width, the latter of which has been described as a key innovation in *Anolis*. [Adaptive radiation; introgression; multispecies network coalescent; phenotypic evolution; phylogenetic network; reticulation; syngameon; transgressive segregation.]

Adaptive radiations provide exceptional opportunities to study the evolution of biodiversity. However, we still have a limited understanding of the conditions that allow for and promote them. Evidence suggests that ecological opportunity, the availability of resources that are evolutionarily accessible, plays a central role in setting the stage for adaptive radiation (Schluter 2000; Mahler et al. 2010; Stroud and Losos 2016), but how do species evolve to access these resources, and what are the mechanisms by which lineages diversify to fill open niche space?

One long-overlooked possibility is that hybridization between well-diverged species may seed evolutionary radiations with novel genetic variation that can allow diverging lineages to more easily access novel adaptive peaks (Seehausen 2004; Parsons et al. 2011; Grant and Grant 2019). Indeed, recent evidence from several young adaptive radiations suggests that hybridization can play a central role in adaptive evolution (The Heliconius Genome Consortium 2012; Lamichhaney et al. 2015; Chaves et al. 2016; Meier et al. 2017; Malinsky et al. 2018). Two prominent hypotheses describe how hybridization can promote diversification during different phases of adaptive radiation (Seehausen 2004; Gillespie et al. 2020). Under the *hybrid swarm origins* hypothesis, admixture between divergent species prior to adaptive radiation triggers the onset of ecological diversification (Seehausen 2004). Under the *syngameon*

hypothesis, admixture between non-sister species within an ongoing adaptive radiation facilitates further adaptive diversification (Seehausen 2004). When hybridization occurs, another open question remains as to whether hybrids exhibit traits that are intermediate to those of their parent species or whether introgression can lead to novel phenotypes outside of parental trait space (Stelkens et al. 2009; Parsons et al. 2011). This latter scenario, termed transgressive evolution, is particularly interesting for the study of adaptive radiation because it may explain how some lineages rapidly diversify into a wide variety of novel forms.

Here, we test for signatures of hybridization and introgression in the adaptive radiation of *Anolis* lizards on Puerto Rico. The Puerto Rican anoles provide an exceptional system in which to explore how and when hybridization contributes to adaptive radiation—the radiation contains a moderate number of species, making it amenable to methods for detecting hybridization, but presents multiple representatives of 3 different *Anolis* ecomorphs—species sharing similar morphological and behavioral adaptations to a particular ecological niche (Losos 2009)—providing opportunities to examine whether ecomorphs have evolved repeatedly within this radiation and whether hybridization occurs within or between ecomorphs. Ten *Anolis* species occur on Puerto Rico (Losos 2009), including 1 crown-giant ecomorph (*A. cuvieri*), 1 twig ecomorph (*A. occultus*),

2 trunk-crown species (*A. evermanni* and *A. stratulus*), 3 trunk-ground anoles (*A. cooki*, *A. cristatellus*, and *A. gundlachi*), and 3 grass-bush species (*A. krugi*, *A. poncensis*, and *A. pulchellus*). This fauna is composed of 3 distinct anole lineages, which likely reached the island independently: *A. occultus*, *A. cuvieri*, and the *cristatellus* series, which contains 8 species that diversified *in situ* on Puerto Rico (Brandley and de Queiroz 2004; Mahler et al. 2010). With the exception of 2 dry-forest specialists (*A. cook* and *A. poncensis*) restricted to the island's southwestern coast (Schwartz and Henderson 1991), all Puerto Rican anole species occur broadly across the island, providing ample opportunities for hybridization. However, hybridization among *Anolis* lizards is presumed to be rare (Losos 2009; Myers et al. 2021), and hybridization among the Puerto Rican anoles has only been suggested for a single pair of species (Jezkova et al. 2013).

We conducted phylogenetic and multispecies network coalescent (MSNC) analyses of genome-wide sequence data from all 10 species of Puerto Rican *Anolis* to examine support for the predictions of the *hybrid swarm* and *syngameon* hypotheses. We also investigated the evolution of the ecomorph classes on Puerto Rico and examined whether introgression occurred between different ecomorphs. Finally, to better understand the role of hybridization in facilitating adaptive radiation, we tested for signals of transgressive evolution in ecologically important traits.

Methods

Whole Genome Sequencing

We collected specimens of *A. cuvieri*, *A. evermanni*, *A. krugi*, *A. gundlachi*, *A. pulchellus*, *A. occultus*, and *A. stratulus* from Puerto Rico and preserved liver tissue in RNAlater solution for genetic analysis. We acquired ethanol-preserved liver tissue for *A. cooki* and *A. poncensis* from the UC Berkeley Museum of Vertebrate Zoology (specimens MVZ226166 and MVZ235170).

We obtained paired-end Illumina data from the NCBI Sequence Read Archive for 1 Puerto Rican species, *A. cristatellus* (SRX2159668), and for an outgroup species, *A. frenatus* (PRJNA400786), in the clade that is sister to the Greater Antillean anoles (Poe et al. 2017). For the remaining 9 Puerto Rican species, we extracted DNA from liver tissue using DNeasy tissue extraction kits (Qiagen Sciences, Germantown, MD, USA) and prepared whole genomic libraries using KAPA HyperPlus kits with enzymatic fragmentation (Roche AG, Basel, Switzerland). We quality checked library size distribution and concentration using a BioAnalyzer 2100 (Agilent Technologies, Santa Clara, CA, USA) and quantified the concentration of dsDNA in prepared libraries using a Qubit 3 fluorometer (Thermo Fisher Scientific, Waltham, MA, USA). Libraries were pooled using results from these 2 assays as well as qPCR. We sequenced samples on partial lanes of Illumina HiSeq 4000 and NovaSeq 6000. For each sample, we generated 20–30Gb of raw read data.

Bioinformatics

We used fastQC (Andrews 2010) to assess read quality and then Trimmomatic (Bolger et al. 2014) to remove low complexity reads and polymerase chain reaction duplicates and Bowtie2 (Langmead and Salzberg 2012) to remove contaminants. We removed adapters using a 4-step procedure in Trimmomatic (Bolger et al. 2014) and cutadapt (Martin 2011). We used FLASH (Magoč and Salzberg 2011) and COPE (Liu et al. 2012) to merge mate pairs and cd-hit (Li and Godzik 2006) for clustering; we applied stringent criteria in this process, retaining only merged reads with phred quality scores above 33. Although this reduced our overall depth of coverage, we set this threshold to ensure high confidence in the retained reads. We mapped the cleaned reads of each sample to the AnoCar2 (Alföldi et al. 2011) genome assembly using BWA-MEM (Li and Durbin 2009) and used SAMtools (Li et al. 2009) to convert, sort, and index the files in bam format. We used bcftools (Li 2011) to call a consensus sequence, followed by the "vcf2fq" function and then "seqtk"(Li 2021) for conversion to fasta format.

To generate genome-wide SNPs and genotype inferences from the bam files, we used "mpileup" (Li et al. 2009) to generate a multi-sample VCF file that retained the mapping quality, used a minimum base quality score of 20, counted orphans, retained read depth, calculated base quality on the fly, and computed genotype likelihoods. We then used SNPcleaner v2.2.4 (Linderoth 2021) to filter variant sites, applying an even coverage filter controlling for exceptionally high or low read depth in any sample and an exact test of Hardy–Weinberg equilibrium with a minimum P-value of 1×10^{-4} (Fumagalli et al. 2014). For the sites that passed filtering, we used ANGSD (Korneliussen et al. 2014) for Bayesian SNP and individual genotype calling using a folded site frequency spectrum, minimum coverage depth of 27x to ensure robust variant calls, and the AnoCar2 reference genome (Alföldi et al. 2011). We set a P-value threshold of 1×10^{-6} for calling SNPs and a 0.95 posterior probability threshold for calling genotypes.

Species Tree Phylogenetic Analysis

We subset our whole genomes by extracting 1809 loci previously identified for their phylogenetic utility, including ultra-conserved elements (UCEs; [Faircloth et al. 2012]), anchored hybrid enrichment loci (AHEs; [Lemmon et al. 2012]), and rapidly evolving long exon capture loci (RELEC; [Karin et al. 2020]). We used SuperCRUNCH (Portik and Wiens 2020) to generate and trim MAFFT (Katoh et al. 2002) alignments for each locus and then generated rapid bootstrapped RAxML gene trees using RaxML v8.0 (Stamatakis 2006; Stamatakis et al. 2008). We then used these gene

trees to estimate a species tree using the accurate species tree algorithm in ASTRAL-III (Zhang et al. 2018). ASTRAL utilizes a multispecies coalescent model that incorporates incomplete lineage sorting and finds the species tree stemming from bipartitions predefined by the gene trees. Branch support for the species tree was assessed with local posterior probabilities, and branch lengths were presented in coalescent units, where shorter branch lengths indicate greater gene tree discordance (Sayyari and Mirarab 2016). To further evaluate uncertainty across the tree (Thomson and Brown 2022), we also calculated gene concordance factors (gCF), defined as the percentage of decisive gene trees containing a given branch (Minh et al. 2020), using IQ-TREE (Nguyen et al. 2015).

D and f Statistics

To evaluate overall departures from tree-like species relationships, we calculated D and f statistics using genome-wide SNPs in ANGSD (Korneliussen et al. 2014) and Dsuite (Malinsky et al. 2021). First, we generated genome-wide Patterson's D statistics (Green et al. 2010; Durand et al. 2011) using ANGSD (Korneliussen et al. 2014) and calculated z-scores using a block jackknife procedure (Green et al. 2010; Durand et al. 2011). We used these to generate the D_{min} statistic (Malinsky et al. 2018) for all species triads without any *a priori* assumptions about their relationships, using *Anolis frenatus*, a mainland species, as the outgroup (Poe et al. 2017). The D_{min} statistic represents the minimum absolute value of Patterson's D for each triad across all possible topologies, with D_{min} scores significantly greater than zero indicating an excess of shared derived alleles between the 3 species that is inconsistent with a single tree topology, even in the presence of incomplete lineage sorting (Malinsky et al. 2018).

To further substantiate the results of the D statistics, we used the f_4 ratio test, which evaluates excess allele sharing (Reich et al. 2009) and the proportion of introgression in the genome among 2 sets of sister taxa (Reich et al. 2009; Martin et al. 2015). For these analyses, using Dsuite (Malinsky et al. 2021), we ran species combinations [f (A, B; C, O)] for all comparisons consistent with the phylogenetic relationships recovered for ((A, B), C) in our ASTRAL tree (Green et al. 2010) and fixed the outgroup to the mainland species, *A. frenatus*. We calculated the f-branch (f_b) metric (Malinsky et al. 2018) to interpret the f_4 ratio tests within their phylogenetic framework so that we could identify evidence of gene flow to specific branches. The f_b statistic (Malinsky et al. 2018) summarizes f scores (Green et al. 2010; Durand et al. 2011) on a given tree to capture excess allele sharing between a species and a specific branch relative to that branch's sister lineage. The f_b statistics are calculated as $f_b(C)$: f (C) = median[min [f (A, B; C, O)]], where B are samples descending from branch b, and A are samples descending from the sister branch of b (Malinsky et al. 2018).

Multispecies Network Coalescent Analysis

We reconstructed phylogenetic networks that allowed for reticulation between branches using 3 multispecies network coalescent (MSNC) approaches: the species networks applying quartets (SNaQ) method implemented in PhyloNetworks (Solís-Lemus and Ané 2016; Solís-Lemus et al. 2017), the maximum pseudo-likelihood method (MPL) implemented in PhyloNet (Than et al. 2008; Wen et al. 2018), and the NeighbourNet-based quartet distance algorithm implemented in NANUQ (Allman et al. 2019). All 3 methods can estimate reticulate phylogenetic networks in the presence of incomplete lineage sorting, even for rapidly diverging species with complex demographics (Yu and Nakhleh 2015; Solís-Lemus and Ané 2016). SNaQ and PhyloNet each return estimates of model fit for an inferred network, based on maximum pseudo-likelihood, and inheritance proportions (γ) for each hybridization event. NANUQ, instead of relying on pseudo-likelihood, estimates network quartet distances between taxa and returns a splits graph and statistics on the quartet topology counts (Allman et al. 2019).

SNaQ estimates a species network based on observed quartet concordance factors (CFs), where quartets are unrooted 4-taxon trees and a quartet's CF is the proportion of genes for which the inferred network displays that quartet (Solís-Lemus and Ané 2016). We estimated CFs directly from our set of 1809 RAxML trees using the "countquartetsintrees" function in PhyloNetworks (Solís-Lemus and Ané 2016). We then used the "snaq!" function to sequentially estimate networks with 0 to 9 possible reticulations, using the ASTRAL tree as the starting tree, enforcing rooting at the outgroup, and updating the network to allow 1 additional reticulation at each step ($h = 0$ to $h = 9$). We identified the optimal number of reticulations by applying a slope heuristic based on the log-likelihood scores for each value of h, as recommended (Solís-Lemus and Ané 2016). For the optimal inferred network, we then performed bootstrapping with 100 replicates using the "bootsnaq" function to estimate support for all branches and reticulations in the network. We also examined support for networks with different values of h using a recently developed goodness-of-fit test (Cai and Ané 2021). This test quantifies the fit between observations from multi-locus data and patterns expected under the multispecies coalescent on candidate phylogenetic networks by comparing the distributions of gene tree topologies for species quartets to those expected under a given network (Cai and Ané 2021). We performed the tests with the QuartetNetworkGoodnessFit Julia package (Cai and Ané 2021), using optimized branch lengths and 1000 simulations of z-values for each network.

The MPL network search implemented in PhyloNet estimates a phylogenetic network based on the frequencies of rooted triples, 3-taxon subtrees, across a set of gene trees (Yu and Nakhleh 2015). We ran the analysis using the "InferNetworkMPL" command in PhyloNet (Than et al. 2008; Wen et al. 2018), using our

set of 1809 RAxML gene trees and allowing for 0 to 5 possible reticulations ($h = 0$ to $h = 5$). For each value of h, we performed 10 independent runs and set a bootstrap threshold of 70 for collapsing branches and reticulations without sufficient support. We identified the optimal number of reticulations by applying a slope heuristic based on the total log probability for each value of h.

The algorithm implemented in NANUQ calculates empirical quartet counts from gene tree topologies for all subsets of 4 taxa, applies a hypothesis test to these counts to determine whether the quartet network displays a 4-cycle, uses the test results to estimate the quartet network distances between taxa, and then constructs a splits graph from the quartet distances (Allman et al. 2019). We ran the analysis in the MSCquartets R package (Rhodes et al. 2021), using our set of 1809 RAxML gene trees with a small value of $\alpha = 10^{-6}$ and a large value of $\beta = 0.95$ as recommended to provide conservative tests for calculating the NANUQ distances (Allman et al. 2019). We visualized the resulting splits graph using SplitsTree4 (Huson and Bryant 2006).

Likelihood Ratio Tests of Speciation with Gene Flow

To further examine signals of potential hybridization, we also tested 3 hypotheses regarding the role of gene flow in speciation for the *Anolis* lizards on Puerto Rico using likelihood ratio tests (LRTs) of speciation with gene flow (Yang 2010), calculated over species divergence times estimated from across the genome. These tests are devised to differentiate between 2 models of speciation with gene flow versus a null model of speciation without gene flow (Yang 2010; Zhu and Yang 2012; Liu et al. 2015; Dalquen et al. 2017). We implemented these analyses in 3s (Yang 2010; Zhu and Yang 2012; Dalquen et al. 2017) using our 1809 extracted loci. We tested a model without gene flow (M_0) against 2 models with gene flow. The first (M_1) approximates a situation in which gene flow decreases after speciation and the migration rate is variable over time (Liu et al. 2015); the second (M_2) is an isolation-with-migration model (Zhu and Yang 2012; Dalquen et al. 2017). We generated pairwise species comparisons with *Anolis frenatus* as the outgroup taxon for all pairs of species, recognizing that results for non-sister taxa reflect the history of divergence extending back to their most recent common ancestor. For each comparison, we re-aligned each locus and removed loci for which any of the 3 focal taxa were missing. We ran the Gaussian quadrature using 32 points for all analyses, ensured that there was proper mixing of the Gaussian equations by discarding runs that yielded highly negative $2\Delta\ell$ values, and then replicated all analyses for consistency.

Transgressive Evolution

Whether hybridization plays a role in facilitating adaptive radiation depends on whether it leads to hybrid lineages accessing novel trait space either through unique combinations of parental traits or by evolving trait values outside of the range occupied by their parental lineages (Seehausen 2004; Parsons et al. 2011). To examine the course of morphological evolution in the Puerto Rican anoles, we reconstructed ancestral states for 5 ecologically important morphological traits, snout-vent length (SVL), head length, femur length, hindtoe IV lamella width, and tail length (Mahler et al. 2010), based on our inferred phylogenetic network, and then tested for transgressive evolution, wherein the trait of a hybrid species is observed to be outside of the range of its 2 parents (Bastide et al. 2018).

We first estimated the trait states at internal nodes in our reticulate phylogeny using the method for reconstructing ancestral states under a Brownian motion model on phylogenetic networks implemented in PhyloNetworks (Solís-Lemus et al. 2017; Bastide et al. 2018). We used the "calibrateFromPairwiseDistances!" function in PhyloNetworks to calibrate our inferred phylogenetic network using genetic distances (Bastide et al. 2018). We generated a pairwise distance matrix by rescaling the branch lengths in each gene tree to a median value of 1 to reduce rate variation across loci, following Bastide et al. (2018), and then calculating the mean patristic distance between all pairs of species across the 1499 trees for which all taxa in our data set are represented. We then ran the "ancestralStateReconstruction" function (Bastide et al. 2018) on the calibrated network for each of the 5 morphological traits. We plotted the phylogenetic network with its observed and reconstructed states for each of these traits (head length, lamella width, and tail length) as phenograms using R.

We then tested for transgressive evolution using the method described by Bastide et al. (2018). This approach tests for shifts in trait values immediately following reticulation points, with a signal of transgressive evolution modeled as the hybrid trait value being the weighted average of its parents plus an additional term representing the hybridization event (Bastide et al. 2018). An F-test implemented in the "phyloNetworklm" function in PhyloNetworks tests for a single coefficient term (of transgressive evolution) across hybridization events (H_1) or individual coefficients for each hybridization event (H_2) against a null model in which hybrids inherit traits as a weighted average from their parents (H_0). We ran this test on each of the 5 morphological traits for the 10 Puerto Rican *Anolis* species in our study; we corrected significance values to account for multiple tests using a false-discovery rate control (Benjamini and Hochberg 1995).

Results

Whole Genome Sequencing

After stringent quality control, filtering, and alignment, we retained an average of 42 876 302 sequence

reads per species with a mean phred quality score of 37.5, resulting in 1.7×–5.5× coverage (mean = 3.8×) across the genome for our 10 ingroup taxa (Supplementary Table S1, Supplementary Material, doi.org/10.6078/D15M69). We recovered a total of 4 000 665 SNPs that we called with a minimum threshold of 27x coverage and that were represented in at least 7 species.

Species Tree Phylogenetic Analysis

We generated individual gene trees for 1809 loci previously identified for their phylogenetic utility, including 1517 UCEs (Faircloth et al. 2012), 117 AHEs (Lemmon et al. 2012), and 175 RELEC loci (Karin et al. 2020), which formed the basis for recovering a robust species tree phylogeny (Fig. 1) using the multispecies coalescent method implemented in ASTRAL-III (Zhang et al. 2018). Posterior probabilities calculated in ASTRAL-III indicated strong support for most of the branches in the phylogeny (Fig. 1); however, gene concordance factors (gCF) calculated in IQ-TREE were generally low, ranging from gCF = 5.1 to 25.9, indicating high levels of gene tree discordance consistant with departures from a bifurcating tree structure.

Consistent with previous studies (Mahler et al. 2010, 2016; Gamble et al. 2014), we found that, of the 10 Puerto Rican *Anolis* species, *A. occultus*, a twig ecomorph, is sister to all other species and that *A. cuvieri*, a crown-giant ecomorph, is sister to the remaining 8

species (the *cristatellus* series; Fig. 1). We also recovered 2 pairs of sister species that were identified previously: *A. evermanni* and *A. stratulus*, both trunk-crown anoles, and *A. cooki* and *A. cristatellus*, 2 trunk-ground species. However, instead of finding *A. krugi* and *A. pulchellus* (Mahler et al. 2010), 2 grass-bush anoles, as sister taxa, the ASTRAL topology placed *A. pulchellus* sister to *A. gundlachi*, a trunk-ground anole. The relationships between the 3 trunk-ground and 3 grass-bush species suggest that one, or both, of these ecomorphs evolved multiple times on Puerto Rico (Fig. 1).

D and f Statistics

We found that 67 of 120 possible triads (55.83%) had D_{min} scores that were significantly elevated after Holm–Bonferroni correction (FWER < 0.001; Supplementary Table S2), suggesting the presence of reticulate evolution throughout the Puerto Rican *Anolis* radiation. Among the f_b scores we calculated, 26 of 84 (30.95%) were significantly elevated (Fig. 2; Supplementary Table S3), with particularly high levels of excess allele sharing between *A. stratulus* and *A. cristatellus*, *A. gundlachi* and *A. cristatellus*, *A. pulchellus* and *A. cristatellus*, *A. cooki* and *A. poncensis*, and between *A. krugi* and the stem of the clade containing *A. cristatellus*, *A. cooki*, *A. gundlachi*, *A. poncensis*, and *A. pulchellus* (and a very high level between *A. krugi* and *A. pulchellus* themselves).
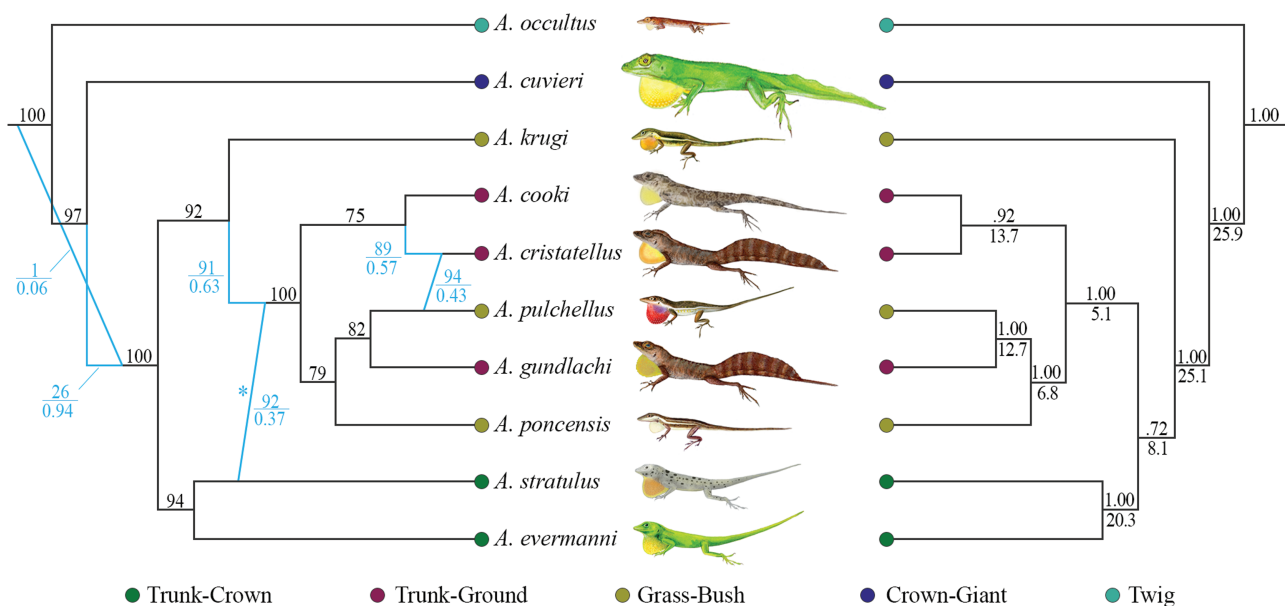

FIGURE 1.   Phylogeny of the Puerto Rican anoles reconstructed using ASTRAL (right) and phylogenetic network inferred using SNaQ and PhyloNet (left). Numbers above branches represent posterior probabilities on the phylogeny (right) and bootstrap support values on the phylogenetic network (left); numbers below branches on the phylogeny (right) indicate gene concordance factors. For the phylogenetic network, blue branches represent inferred reticulations. The numbers above the bars next to these branches indicate bootstrap support values from the SNaQ analysis; the numbers below the bars represent the ancestry proportions (γ) inferred by SNaQ. The asterisk (*) identifies the reticulation that received bootstrap support (>70) in the PhyloNet analysis.
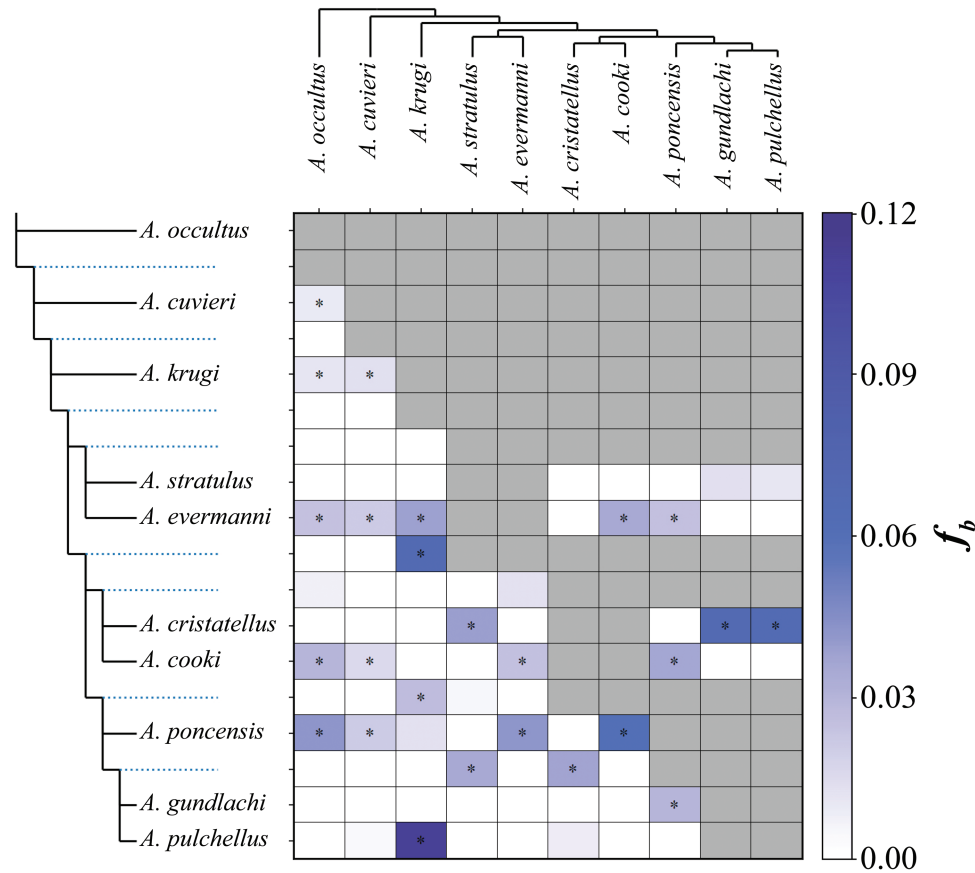
FIGURE 2. Heatmap for pairwise f-branch (f_b) statistics calculated using Dsuite (Dalquen et al. 2017). The f_b statistic represents excess sharing of derived alleles between the branch of the tree on the y-axis (left) and the species on the x-axis (top). Darker colors indicate higher f_b values, and asterisks (*) indicate values that were significantly elevated after Holm-Bonferroni correction (FWER < 0.001). Individual f_b scores are listed in Supplementary Table S3.

Likelihood Ratio Tests of Speciation with Gene Flow

Our LRTs of speciation with gene flow (Yang 2010; Zhu and Yang 2012; Dalquen et al. 2017) found significant signals of decreasing gene flow following speciation between a pair of trunk-ground anoles, *A. cristatellus* and *A. gundlachi* (M_1, $2\Delta\ell = 22.498$), and between *A. pulchellus*, a grass-bush anole, and 2 trunk-ground anoles, *A. cristatellus* (M_1, $2\Delta\ell = 35.527$) and *A. gundlachi* (M_1, $2\Delta\ell = 40.193$). We also found significant support for a model of decreasing gene flow following speciation (M_1, $2\Delta\ell = 56.459$) and a model of isolation-with-migration (M_2, $2\Delta\ell = 55.433$) between *A. cristatellus*, a trunk-ground ecomorph, and *A. evermanni*, a trunk-crown ecomorph (Table S5). Because the LRTs are applied to sets of 3 species at a time and because we used *A. frenatus* as the outgroup for all comparisons, for pairs that are not sister species based on the inferred phylogeny, it is best to interpret the result as applying to the lineages leading to each extant species. We did not find support for models of speciation with gene flow between any other pair of species (Supplementary Table S5).

Multispecies Network Coalescent Analysis

All 3 MSNC methods—SNaQ (Solís-Lemus et al. 2017), PhyloNet (Wen et al. 2018), and NANUQ (Allman et al. 2019)—identified strong support for hybridization events among the 10 species of Puerto Rican anoles (Fig. 1). Based on a slope heuristic applied to log-likelihood scores in SNaQ and total log probabilities in PhyloNet, we found 3 reticulations as the optimal arrangement in SNaQ and 1 reticulation as optimal in our PhyloNet analysis (Supplementary Table S4). SNaQ and PhyloNet both inferred a hybrid edge between *A. stratulus*, a trunk-crown species, and the stem of the clade containing 2 grass-bush species and the 3 trunk-ground species (Fig. 1). Bootstrap analyses in both SNaQ and PhyloNet confirmed support for this hybridization event, and the γ values inferred in SNaQ suggest ancestral proportions of 0.37 from *A. stratulus* and 0.63 from *A. krugi* into the stem of this clade (Fig. 1). Our SNaQ analysis also found bootstrap support for a more recent hybridization between *A. pulchellus*, a grass-bush species, and *A. cooki*, a trunk-ground species, leading to the formation of *A. cristatellus*, a species with remarkably similar

morphology to *A. cooki* (Fig. 1). Finally, SNaQ suggested an older hybridization between the stem or an unsampled lineage outside of the Puerto Rican anoles and *A. cuvieri* (or its ancestor or one of its non-Puerto Rican relatives) into the stem of the *cristatellus* series, but this hybrid edge was not supported by bootstrap analyses (Fig. 1).

Quartet goodness of fit tests (Cai and Ané 2021) also indicated that the SNaQ network with 3 reticulations had the best fit to our data of the 10 networks we evaluated ($z/\sigma = 13.81$, $P = 1.11 \times 10^{-43}$). All of the networks with at least 1 reticulation provided more adequate models ($z/\sigma = 14.31$ to 15.36, $P = 7.64 \times 10^{-47}$ to 1.42×10^{-77}) than the network with no reticulations ($z/\sigma = 21.55$, $P = 8.28 \times 10^{-107}$). However, all of our candidate networks exhibited some level of inadequacy, with the significant model *P*-values indicating departures from the expected distribution of outlier quartet *P*-values (quartets exhibiting discordance from the candidate network), suggesting that the history of reticulation among the Puerto Rican *Anolis* may be even more complex than a network with 3 hybridization events.

The splits graph we recovered from NANUQ is broadly consistent with these results (Supplementary Fig. S1). A simplex plot of the quartet hypothesis tests indicates a large number of departures from a strict tree structure among quartet topologies, and the splits graph itself exhibits many parallel edges and alternative splits between taxa (Supplementary Fig. S1). The graph also contains a large number of 4-cycles, particularly among the *cristatellus* series taxa, which is consistent with a pattern of reticulate evolution.

Transgressive Evolution

We found significant signals of transgressive evolution for lamella width ($P = 0.023$) and head length traits ($P = 0.009$) that were homogeneous (H_1) across the 2 inferred hybridization events that had strong bootstrap support (Supplementary Fig. S2; Supplementary Table S6), indicating a shift in trait values immediately following hybrid nodes (Bastide et al. 2018). We did not find statistically significant evidence for transgressive evolution in body size (SVL), femur length, or tail length (Supplementary Table S6).

Discussion

Our analyses of genome-wide variation in the ten species of Puerto Rican *Anolis* lizards revealed multiple lines of evidence for introgression across this adaptive radiation. We detected hybridization not only between extant species but also deeper in the Puerto Rican *Anolis* tree, and we found evidence for introgression between different ecomorphs as well. These hybridization events were associated with significant signals of transgressive evolution, in which admixed lineages access phenotypic space outside of the ranges of their parental lineages, suggesting that hybridization may have played

an important role in generating phenotypic diversity during this adaptive radiation.

We found equivocal support for the *hybrid swarm origins* hypothesis, in which admixture prior to the beginning of an adaptive radiation triggers diversification (Seehausen 2004); the phylogenetic networked inferred by SNaQ identified a small, asymmetric reticulation event prior to the onset of *in situ* diversification on Puerto Rico, but this reticulate edge was not bootstrap-supported nor identified in the optimal PhyloNet topology (Fig. 1). However, our analyses did reveal strong support for the *syngameon* hypothesis of adaptive radiation, under which hybridization between non-sister lineages within an adaptive radiation facilitates further ecological divergence and speciation (Seehausen 2004; Gillespie et al. 2020). Both SNaQ and PhyloNet inferred a strongly supported hybrid origin for a lineage within the *cristatellus* series, resulting from introgression between *A. krugi* ($\gamma = 0.63$) and *A. stratulus* ($\gamma = 0.37$), that later diversified into 5 species (Fig. 1). Another recent study found evidence of hybridization between a pair of *Anolis* species in the Jamaican radiation that occurred in the recent past and did not lead to subsequent diversification (Myers et al. 2021). By contrast, our results suggest diversification immediately downstream of a hybridization event that occurred deeper in the phylogeny, adding to a growing body of evidence that ancient hybridization events may, at least in some cases, be linked to adaptive radiation (Meier et al. 2017; Gillespie et al. 2020). Our MSNC result was also supported by significantly elevated D_{min} and f_b scores between *A. krugi*, *A. stratulus*, and the 5 species that make up the hybrid clade (Fig. 2; Supplementary Table S1), which also exhibited a network structure consistent with reticulate evolution in our NANUQ results (Supplementary Fig. S1). This clade comprises 2 different ecomorphs and includes the initial (and potentially the second) origin of the trunk-ground ecomorph on Puerto Rico, suggesting that this hybridization event may have contributed to ecomorphological diversification.

Under the *syngameon* hypothesis, hybridization acts as a creative force that can allow hybrid lineages to access novel trait space, an essential component for adaptive radiation (Seehausen 2004; Gillespie et al. 2020). Greater divergence between species prior to hybridization increases the potential for hybridization to introduce novel and advantageous recombinant genotypes and structural variants, leading to phenotypic novelty (Seehausen 2004; Stelkens et al. 2009). Our phylogenetic analyses and ancestral state reconstructions suggest that the ancestors for *A. krugi* and *A. stratulus* had already undergone some morphological divergence at their time of hybridization, potentially contributing to the burst of adaptive diversification following this event. This pattern joins recent discoveries in systems ranging from Hawaiian silverswords to Darwin's finches (Friar et al. 2008; Lamichhaney et al. 2015) to suggest that hybridization between non-sister lineages is potentially a common facet in the evolution

of adaptive radiations (Feder et al. 2003; Merrill et al. 2015; Meier et al. 2017). In fact, hybridization increasingly appears to play an important role in the evolution of biodiversity in general (Eberlein et al. 2019; Martin et al. 2019; Nieto Feliner et al. 2020).

Fundamentally, the *syngameon* concept describes a complex of species linked by introgression. Among the Puerto Rican anoles, we found that 56% of D_{min} statistics and 31% of f_b statistics were significantly elevated (Fig. 2; Supplementary Table S1), indicating excess allele sharing between species that is inconsistent with tree-like species relationships (Green et al. 2010; Durand et al. 2011; Malinsky et al. 2018). The highest f_b score we found was between *A. krugi* and *A. pulchellus*, 2 grass-bush anoles, consistent with previous research that found mtDNA introgression from *A. krugi* into *A. pulchellus* (Jezkova et al. 2013). The concordance of these findings lends support to the role of introgression in this radiation, and our results suggest that introgression between *A. krugi* and *A. pulchellus* is not limited to mtDNA. These 2 species exhibit very similar morphologies (Fig. 1), use similar microhabitats, and overlap broadly in their ranges across Puerto Rico (Schwartz and Henderson 1991; Jezkova et al. 2013). Although *A. krugi* is often associated with shaded habitat, while *A. pulchellus* tends to prefer open habitat (Schwartz and Henderson 1991; Jezkova et al. 2013), the 2 regularly occur in syntopy across the island where these habitats meet (Jezkova et al. 2013).

The phylogenetic network inferred by SNaQ also identified a potential hybridization event between *A. pulchellus*, a grass-bush anole, and *A. cooki*, a trunk-ground anole, that resulted in a hybrid origin for *A. cristatellus*, a trunk-ground anole (Fig. 1). This reticulation was not recovered by PhyloNet, but our LRTs of speciation with gene flow did identify significant support for a model of gene flow following speciation between the lineages leading to *A. cristatellus* and *A. pulchellus*, and we found a significant and highly elevated f_b score (f_b = 0.068, $P < 1 \times 10^{-6}$) that suggests introgression from *A. pulchellus* to *A. cristatellus*. A potential hybrid origin for *A. cristatellus* is intriguing given that it has the broadest distribution of the 3 Puerto Rican trunk-ground anoles, shows substantial phenotypic variation between populations, and is abundant across a broad range of habitats (Schwartz and Henderson 1991). The 2 other trunk-ground species, on the other hand, are more geographically restricted and habitat specific, with *A. cooki* only found in the dry forests along the southwest coast and *A. gundlachi* primarily occurring in mid- to high-elevation, closed, mesic forest (Schwartz and Henderson 1991).

The speciation with gene flow LRTs also recovered significant signals of gene flow following speciation between the ancestors of *A. cristatellus* and *A. gundlachi* (M_1, $2\Delta\ell$ = 35.527) and between *A. gundlachi* and *A. pulchellus* (M_1, $2\Delta\ell$ = 40.193). We also found a significantly elevated f_b score suggesting introgression between *A. gundlachi* and *A. cristatellus* (f_b = 0.070, $P < 1 \times 10^{-6}$; Fig. 2; Supplementary Table S2); there are no f_b statistics for

A. gundlachi and *A. pulchellus* because they are sister species. Hence, in combination, the MSNC analyses, f_b statistics, and speciation with gene flow LRTs suggest that these 3 species exhibit departures from tree-like structure consistent with introgression. These species all overlap broadly across Puerto Rico and are all locally abundant. The 2 trunk-ground species, *A. cristatellus* and *A. gundlachi*, exhibit very similar morphologies overall—the primary distinguishing characters are a blue iris, yellow coloration under the chin, and entirely yellow dewlap in *A. gundlachi* (compared to a 2-tone greenish-yellow and orange dewlap in *A. cristatellus*)—and the 2 species are often found nearby, although *A. gundlachi* prefers closed forest habitat compared to *A. cristatellus* (Schwartz and Henderson 1991). The 2 other species in the clade with these 3, *A. cooki*, sister to *A. cristatellus*, and *A. poncensis*, sister to *A. gundlachi* and *A. pulchellus* (Fig. 1), are both restricted to dry-forest habitat (Schwartz and Henderson 1991). This topology suggests that dry-forest specialization in these species evolved independently and that the trunk-ground ecomorph evolved twice in the Puerto Rican radiation (or that there were multiple shifts between grass-bush and trunk-ground ecomorphology; Fig. 1). Evidence for introgression between extant taxa along with a strongly supported reticulation event deeper in the tree also suggest that hybridization may have taken place across different stages of the adaptive radiation of *Anolis* on Puerto Rico.

Finally, whether hybridization plays a role in facilitating adaptive radiation depends on whether it leads to hybrid lineages evolving more rapidly or accessing novel trait space, either through unique combinations of parental traits or by evolving trait values outside of the range occupied by their parental lineages (Seehausen 2004; Parsons et al. 2011). Although our tests for transgressive evolution did not identify this pattern in limb or tail dimensions, we did detect significant signals of transgressive evolution for lamella width and head length traits, indicating evolutionary shifts in the values of these traits following hybrid nodes that were not explained by weighted parental values alone (Bastide et al. 2018). These results are consistent with the hypothesis that hybridization may have contributed to adaptive radiation in *Anolis* through the evolution of phenotypic novelty.

Both traits are associated with ecological diversification and microhabitat specialization in *Anolis* (Losos 2009). Head traits are associated with differences in feeding ecology, mainly through changes in bite force that influence foraging behavior and prey selection (Herrel et al. 2006). Lamellae, which underlie the adhesive properties of *Anolis* toepads, drive clinging and climbing performance (Irschick et al. 2006), and their differences are associated with fine-scale vertical habitat partitioning (Yuan et al. 2019). They are so important to the utilization of arboreal niche space, in fact, that toepads have been proposed as a key innovation in *Anolis* (Warheit et al. 1999; Losos 2009; Burress and Muñoz 2021). Hence, our results

suggest that hybridization contributed to the evolution of phenotypic diversity in key traits that drove ecological diversification in the adaptive radiations of anoles. This finding suggests that transgressive evolution may provide a key mechanism by which hybridization facilitates adaptive radiation by generating diversity through the evolution of phenotypic novelty. In theory, such transgressive segregation during hybridization may allow lineages to cross fitness valleys (Kagawa and Takimoto 2018; Marques et al. 2019), rapidly acquire novel phenotypic diversity (Parsons et al. 2011; Husemann et al. 2017), and access new ecological niches (Kagawa and Takimoto 2018).

Conclusions

Multiple analyses uncovered signals of introgression across the Puerto Rican *Anolis* tree, including hybridization between different ecomorphs and between non-sister species that led to further diversification, satisfying the principal predictions of the *syngameon* hypothesis. Evidence for the *syngameon* hypothesis has been identified in the adaptive radiations of cichlids (Meier et al. 2017), Darwin's finches (Lamichhaney et al. 2015), *Rhagoletis* flies (Feder et al. 2003), *Heliconius* butterflies (Merrill et al. 2015), and silverswords (Friar et al. 2008), and our findings further suggest this mechanism plays an important role in adaptive radiation. Moreover, we found that hybridization was associated with transgressive evolution for 2 ecologically important traits, head length and toepad width, which has been identified as a key innovation contributing to adaptive radiation in *Anolis* (Losos 2009; Burress and Muñoz 2021). Hence, altogether, our results suggest that introgression occurred during multiple stages of the Puerto Rican *Anolis* radiation and that hybridization can, indeed, facilitate evolution into novel phenotypic space during adaptive radiation.

Supplementary Material

Data available from the Dryad Digital Repository: http://dx.doi.org/10.6078/D15M69.

Data Availability

The raw sequence read data generated under this project are available from the NCBI Sequence Read Archive (BioProject PRJNA949240). The data files needed to reproduce the analyses presented here are available from the Dryad data repository at http://datadryad.org, doi.org/10.6078/D15M69.

References

Alföldi J., Di Palma F., Grabherr M., Williams C., Kong L., Mauceli E., Russell P., Lowe C.B., Glor R.E., Jaffe J.D., Ray D.A., Boissinot S., Shedlock A.M., Botka C., Castoe T.A., Colbourne J.K., Fujita M.K., Moreno R.G., ten Hallers B.F., Haussler D., Heger A., Heiman D., Janes D.E., Johnson J., de Jong P.J., Koriabine M.Y., Lara M., Novick P.A., Organ C.L., Peach S.E., Poe S., Pollock D.D., de Queiroz K., Sanger T., Searle S., Smith J.D., Smith Z., Swofford R., Turner-Maier J., Wade J., Young S., Zadissa A., Edwards S.V., Glenn T.C., Schneider C.J., Losos J.B., Lander E.S., Breen M., Ponting C.P., Lindblad-Toh K. 2011. The genome of the green anole lizard and a comparative analysis with birds and mammals. Nature 477:587–591.

Allman E.S., Baños H., Rhodes J.A. 2019. NANUQ: a method for inferring species networks from gene trees under the coalescent model. Algorithms Mol. Biol. 14:24.

Andrews S. 2010. FastQC: a quality control tool for high throughput sequence data. Available online at: http://www.bioinformatics.babraham.ac.uk/projects/fastqc/

Bastide P., Solís-Lemus C., Kriebel R., William Sparks K., Ané C. 2018. Phylogenetic comparative methods on phylogenetic networks with reticulations. Syst. Biol. 67:800–820.

Benjamini Y., Hochberg Y. 1995. Controlling the false discovery rate: a practical and powerful approach to multiple testing. J. R. Stat. Soc. Ser. B Methodol. 57:289–300.

Bolger A.M., Lohse M., Usadel B. 2014. Trimmomatic: a flexible trimmer for Illumina sequence data. Bioinformatics. 30: 2114–2120.

Brandley M.C., de Queiroz K. 2004. Phylogeny, ecomorphological evolution, and historical biogeography of the *Anolis cristatellus* series. Herpetol. Monogr. 18:90–126.

Burress E.D., Muñoz M.M. 2021. Ecological opportunity from innovation, not islands, drove the anole lizard adaptive radiation. Syst. Biol.: syab031.

Cai R., Ané C. 2021. Assessing the fit of the multi-species network coalescent to multi-locus data. Bioinformatics 37:634–641.

Chaves J.A., Cooper E.A., Hendry A.P., Podos J., León L.F.D., Raeymaekers J.A.M., MacMillan W.O., Uy J.A.C. 2016. Genomic variation at the tips of the adaptive radiation of Darwin's finches. Mol. Ecol. 25:5282–5295.

Dalquen D.A., Zhu T., Yang Z. 2017. Maximum likelihood implementation of an isolation-with-migration model for three species. Syst. Biol. 66:379–398.

Durand E.Y., Patterson N., Reich D., Slatkin M. 2011. Testing for ancient admixture between closely related populations. Mol. Biol. Evol. 28:2239–2252.

Eberlein C., Hénault M., Fijarczyk A., Charron G., Bouvier M., Kohn L.M., Anderson J.B., Landry C.R. 2019. Hybridization is a recurrent evolutionary stimulus in wild yeast speciation. Nat. Commun. 10:923.

Faircloth B.C., McCormack J.E., Crawford N.G., Harvey M.G., Brumfield R.T., Glenn T.C. 2012. Ultraconserved elements anchor thousands of genetic markers spanning multiple evolutionary timescales. Syst. Biol. 61:717–726.

Feder J.L., Berlocher S.H., Roethele J.B., Dambroski H., Smith J.J., Perry W.L., Gavrilovic V., Filchak K.E., Rull J., Aluja M. 2003. Allopatric genetic origins for sympatric host-plant shifts and race formation in *Rhagoletis*. Proc. Natl. Acad. Sci. 100:10314–10319.

Friar E.A., Prince L.M., Cruse-Sanders J.M., McGlaughlin M.E., Butterworth C.A., Baldwin B.G. 2008. Hybrid origin and genomic mosaicism of *Dubautia scabra* (Hawaiian silversword alliance; Asteraceae, Madiinae). Syst. Bot. 33:589–597.

Fumagalli M., Vieira F.G., Linderoth T., Nielsen R. 2014. ngsTools: methods for population genetics analyses from next-generation sequencing data. Bioinformatics 30:1486–1487.

Gamble T., Geneva A.J., Glor R.E., Zarkower D. 2014. *Anolis* sex chromosomes are derived from a single ancestral pair. Evolution 68:1027–1041.

Gillespie R.G., Bennett G.M., De Meester L., Feder J.L., Fleischer R.C., Harmon L.J., Hendry A.P., Knope M.L., Mallet J., Martin C., Parent C.E., Patton A.H., Pfennig K.S., Rubinoff D., Schluter D., Seehausen O., Shaw K.L., Stacy E., Stervander M., Stroud J.T., Wagner C., Wogan G.O.U. 2020. Comparing adaptive radiations across space, time, and taxa. J. Hered. 111:1–20.

Grant P.R., Grant B.R. 2019. Hybridization increases population variation during adaptive radiation. Proc. Natl. Acad. Sci. 116:23216–23224.

Green R.E., Krause J., Briggs A.W., Maricic T., Stenzel U., Kircher M., Patterson N., Li H., Zhai W., Fritz M.H.-Y., Hansen N.F., Durand E.Y., Malaspinas A.-S., Jensen J.D., Marques-Bonet T., Alkan C., Prüfer K., Meyer M., Burbano H.A., Good J.M., Schultz R., Aximu-Petri A., Butthof A., Höber B., Höffner B., Siegemund M., Weihmann A., Nusbaum C., Lander E.S., Russ C., Novod N., Affourtit J., Egholm M., Verna C., Rudan P., Brajkovic D., Kucan Ž., Gušic I., Doronichev V.B., Golovanova L.V., Lalueza-Fox C., de la Rasilla M., Fortea J., Rosas A., Schmitz R.W., Johnson P.L.F., Eichler E.E., Falush D., Birney E., Mullikin J.C., Slatkin M., Nielsen R., Kelso J., Lachmann M., Reich D., Pääbo S. 2010. A draft sequence of the Neandertal genome. Science. 328:710–722.

The Heliconius Genome Consortium. 2012. Butterfly genome reveals promiscuous exchange of mimicry adaptations among species. Nature 487:94–98.

Herrel A., Joachim R., Vanhooydonck B., Irschick D.J. 2006. Ecological consequences of ontogenetic changes in head shape and bite performance in the Jamaican lizard *Anolis lineatopus*. Biol. J. Linn. Soc. 89:443–454.

Husemann M., Tobler M., McCauley C., Ding B., Danley P.D. 2017. Body shape differences in a pair of closely related Malawi cichlids and their hybrids: Effects of genetic variation, phenotypic plasticity, and transgressive segregation. Ecol. Evol. 7:4336–4346.

Huson D.H., Bryant D. 2006. Application of phylogenetic networks in evolutionary studies. Mol. Biol. Evol. 23:254–267.

Irschick D.J., Herrel A., Vanhooydonck B. 2006. Whole-organism studies of adhesion in pad-bearing lizards: creative evolutionary solutions to functional problems. J. Comp. Physiol. A 192:1169–1177.

Jezkova T., Leal M., Rodríguez-Robles J.A. 2013. Genetic drift or natural selection? Hybridization and asymmetric mitochondrial introgression in two Caribbean lizards (*Anolis pulchellus* and *Anolis krugi*). J. Evol. Biol. 26:1458–1471.

Kagawa K., Takimoto G. 2018. Hybridization can promote adaptive radiation by means of transgressive segregation. Ecol. Lett. 21:264–274.

Karin B.R., Gamble T., Jackman T.R. 2020. Optimizing phylogenomics with rapidly evolving long exons: comparison with anchored hybrid enrichment and ultraconserved elements. Mol. Biol. Evol. 37:904–922.

Katoh K., Misawa K., Kuma K., Miyata T. 2002. MAFFT: a novel method for rapid multiple sequence alignment based on fast Fourier transform. Nucleic Acids Res. 30:3059–3066.

Korneliussen T.S., Albrechtsen A., Nielsen R. 2014. ANGSD: analysis of next generation sequencing data. BMC Bioinf. 15:356.

Lamichhaney S., Berglund J., Almén M.S., Maqbool K., Grabherr M., Martinez-Barrio A., Promerová M., Rubin C.-J., Wang C., Zamani N., Grant B.R., Grant P.R., Webster M.T., Andersson L. 2015. Evolution of Darwin's finches and their beaks revealed by genome sequencing. Nature 518:371–375.

Langmead B., Salzberg S.L. 2012. Fast gapped-read alignment with Bowtie 2. Nat. Methods 9:357–359.

Lemmon A.R., Emme S.A., Lemmon E.M. 2012. Anchored hybrid enrichment for massively high-throughput phylogenomics. Syst. Biol. 61:727–744.

Li H. 2011. A statistical framework for SNP calling, mutation discovery, association mapping and population genetical parameter estimation from sequencing data. Bioinformatics 27:2987–2993.

Li H. 2021. lh3/seqtk. Available online at: https://github.com/lh3/seqtkLi

Li H., Durbin R. 2009. Fast and accurate short read alignment with Burrows-Wheeler transform. Bioinforma. Oxf. Engl. 25:1754–1760.

Li H., Handsaker B., Wysoker A., Fennell T., Ruan J., Homer N., Marth G., Abecasis G., Durbin R.; 1000 Genome Project Data Processing Subgroup. 2009. The sequence alignment/map format and SAMtools. Bioinformatics 25:2078–2079.

Li W., Godzik A. 2006. Cd-hit: a fast program for clustering and comparing large sets of protein or nucleotide sequences. Bioinformatics 22:1658–1659.

Linderoth T. 2021. ngsQC. Available online at: https://github.com/tplinderoth/ngsQC

Liu B., Yuan J., Yiu S.-M., Li Z., Xie Y., Chen Y., Shi Y., Zhang H., Li Y., Lam T.-W., Luo R. 2012. COPE: an accurate k-mer-based pair-end reads connection tool to facilitate genome assembly. Bioinformatics 28:2870–2874.

Liu J., Zhang D.-X., Yang Z. 2015. A discrete-beta model for testing gene flow after speciation. Methods Ecol. Evol. 6:715–724.

Losos J.B. 2009. Lizards in an Evolutionary Tree: Ecology and Adaptive Radiation of Anoles. Berkeley, CA: University of California Press.

Magoč T., Salzberg S.L. 2011. FLASH: fast length adjustment of short reads to improve genome assemblies. Bioinformatics 27:2957–2963.

Mahler D.L., Lambert S.M., Geneva A.J., Ng J., Hedges S.B., Losos J.B., Glor R.E. 2016. Discovery of a giant chameleon-like lizard (*Anolis*) on Hispaniola and its significance to understanding replicated adaptive radiations. Am. Nat. 188:357–364.

Mahler D.L., Revell L.J., Glor R.E., Losos J.B. 2010. Ecological opportunity and the rate of morphological evolution in the diversification of Greater Antillean anoles. Evolution 64:2731–2745.

Malinsky M., Matschiner M., Svardal H. 2021. Dsuite - Fast D-statistics and related admixture evidence from VCF files. Mol. Ecol. Resour. 21:584–595.

Malinsky M., Svardal H., Tyers A.M., Miska E.A., Genner M.J., Turner G.F., Durbin R. 2018. Whole-genome sequences of Malawi cichlids reveal multiple radiations interconnected by gene flow. Nat. Ecol. Evol. 2:1940–1955.

Marques D.A., Meier J.I., Seehausen O. 2019. A combinatorial view on speciation and adaptive radiation. Trends Ecol. Evol. 34:531–544.

Martin C.H., McGirr J.A., Richards E.J., St. John M.E. 2019. How to investigate the origins of novelty: insights gained from genetic, behavioral, and fitness perspectives. Integr. Org. Biol. 1:obz018.

Martin M. 2011. Cutadapt removes adapter sequences from high-throughput sequencing reads. EMBnet J 17:10–12.

Martin S.H., Davey J.W., Jiggins C.D. 2015. Evaluating the use of ABBA–BABA statistics to locate introgressed loci. Mol. Biol. Evol. 32:244–257.

Meier J.I., Marques D.A., Mwaiko S., Wagner C.E., Excoffier L., Seehausen O. 2017. Ancient hybridization fuels rapid cichlid fish adaptive radiations. Nat. Commun. 8:14363.

Merrill R.M., Dasmahapatra K.K., Davey J.W., Dell'Aglio D.D., Hanly J.J., Huber B., Jiggins C.D., Joron M., Kozak K.M., Llaurens V., Martin S.H., Montgomery S.H., Morris J., Nadeau N.J., Pinharanda A.L., Rosser N., Thompson M.J., Vanjari S., Wallbank R.W.R., Yu Q. 2015. The diversification of *Heliconius* butterflies: what have we learned in 150 years? J. Evol. Biol. 28:1417–1438.

Minh B.Q., Hahn M.W., Lanfear R. 2020. New methods to calculate concordance factors for phylogenomic datasets. Mol. Biol. Evol. 37:2727–2733.

Myers E.A., Mulcahy D.G., Falk B., Johnson K., Carbi M., de Queiroz K. 2021. Interspecific gene flow and mitochondrial genome capture during the radiation of Jamaican Anolis lizards (Squamata; Iguanidae). Syst. Biol.: syab089.

Nguyen L.-T., Schmidt H.A., von Haeseler A., Minh B.Q. 2015. IQ-TREE: a fast and effective stochastic algorithm for estimating maximum-likelihood phylogenies. Mol. Biol. Evol. 32:268–274.

Nieto Feliner G., Casacuberta J., Wendel J.F. 2020. Genomics of evolutionary novelty in hybrids and polyploids. Front. Genet. 11:792.

Parsons K.J., Son Y.H., Craig Albertson R. 2011. Hybridization promotes evolvability in African cichlids: connections between transgressive segregation and phenotypic integration. Evol. Biol. 38:306–315.

Poe S., Nieto-montes de oca A., Torres-carvajal O., De Queiroz K., Velasco J.A., Truett B., Gray L.N., Ryan M.J., Köhler G., Ayala-varela F., Latella I. 2017. A Phylogenetic, Biogeographic, and Taxonomic study of all Extant Species of Anolis (Squamata; Iguanidae). Syst. Biol. 66:663–697.

Portik D.M., Wiens J.J. 2020. SuperCRUNCH: A bioinformatics toolkit for creating and manipulating supermatrices and other large phylogenetic datasets. Methods Ecol. Evol. 11:763–772.

Reich D., Thangaraj K., Patterson N., Price A.L., Singh L. 2009. Reconstructing Indian population history. Nature 461:489–494.

Rhodes J.A., Baños H., Mitchell J.D., Allman E.S. 2021. MSCquartets 1.0: quartet methods for species trees and networks under the multispecies coalescent model in R. Bioinformatics 37:1766–1768.

Sayyari E., Mirarab S. 2016. Fast coalescent-based computation of local branch support from quartet frequencies. Mol. Biol. Evol. 33:1654–1668.

Schluter D. 2000. The ecology of adaptive radiation. Oxford, UK: Oxford University Press.

Schwartz A., Henderson R.W. 1991. Amphibians and reptiles of the west indies: descriptions, distributions, and natural history. Gainesville, FL: University of Florida Press.

Seehausen O. 2004. Hybridization and adaptive radiation. Trends Ecol. Evol. 19:198–207.

Solís-Lemus C., Ané C. 2016. Inferring phylogenetic networks with maximum pseudolikelihood under incomplete lineage sorting. PLoS Genet. 12:e1005896.

Solís-Lemus C., Bastide P., Ané C. 2017. PhyloNetworks: a package for phylogenetic networks. Mol. Biol. Evol. 34:3292–3298.

Stamatakis A. 2006. RAxML-VI-HPC: maximum likelihood-based phylogenetic analyses with thousands of taxa and mixed models. Bioinformatics 22:2688–2690.

Stamatakis A., Hoover P., Rougemont J. 2008. A rapid bootstrap algorithm for the RAxML web servers. Syst. Biol. 57:758–771.

Stelkens R.B., Schmid C., Selz O., Seehausen O. 2009. Phenotypic novelty in experimental hybrids is predicted by the genetic distance between species of cichlid fish. BMC Evol. Biol. 9:283.

Stroud J.T., Losos J.B. 2016. Ecological opportunity and adaptive radiation. Annu. Rev. Ecol. Evol. Syst. 47:507–532.

Than C., Ruths D., Nakhleh L. 2008. PhyloNet: a software package for analyzing and reconstructing reticulate evolutionary relationships. BMC Bioinf. 9:322.

Thomson R.C., Brown J.M. 2022. On the need for new measures of phylogenomic support. Syst. Biol. 71:917–920.

Warheit K.I., Forman J.D., Losos J.B., Miles D.B. 1999. Morphological diversification and adaptive radiation: a comparison of two diverse lizard clades. Evolution 53:1226–1234.

Wen D., Yu Y., Zhu J., Nakhleh L. 2018. Inferring phylogenetic networks using phyloNet. Syst. Biol. 67:735–740.

Yang Z. 2010. A likelihood ratio test of speciation with gene flow using genomic sequence data. Genome Biol. Evol. 2:200–211.

Yu Y., Nakhleh L. 2015. A maximum pseudo-likelihood approach for phylogenetic networks. BMC Genomics 16:S10.

Yuan M.L., Wake M.H., Wang I.J. 2019. Phenotypic integration between claw and toepad traits promotes microhabitat specialization in the *Anolis* adaptive radiation. Evolution 73:231–244.

Zhang C., Rabiee M., Sayyari E., Mirarab S. 2018. ASTRAL-III: polynomial time species tree reconstruction from partially resolved gene trees. BMC Bioinf. 19:153.

Zhu T., Yang Z. 2012. Maximum likelihood implementation of an isolation-with-migration model with three species for testing speciation with gene flow. Mol. Biol. Evol. 29:3131–3142.